

Article

Mineralogy of Skarn Ores from Băița-Bihor, Northern Apuseni Mountains, Romania: A Case Study of Cu-, Bi-, and Sn-minerals

Călin Gabriel Tămaș  and Mădălina-Paula Andrii * 

Department of Geology, Faculty of Biology and Geology, Babeș-Bolyai University, 1, Mihail Kogălniceanu Str., 400084 Cluj-Napoca, Romania; calin.tamas@ubbcluj.ro

* Correspondence: andrii.madalinapaula@gmail.com

Received: 16 April 2020; Accepted: 12 May 2020; Published: 13 May 2020



Abstract: The Antoniu, Antoniu North, and Blidar Contact orebodies from the Băița-Bihor skarn deposit, Romania have been investigated using optical and electron microscopy. Electron probe microanalyses were acquired on samples from the Blidar Contact orebody. Bornite is the most abundant Cu-sulfide and hosts native bismuth, joséite-B, emplectite, and wittichenite. Kesterite and ferrokesterite were identified for the first time in the Băița-Bihor deposit; the occurrence of stannite was also confirmed. Temperatures of ore deposition in the Blidar Contact orebody are constrained from the compositions of sphalerite-kesterite and sphalerite-ferrokesterite pairs at 287 ± 25 °C to 310 ± 35 °C, and 447 ± 17 °C to 503 ± 68 °C, respectively.

Keywords: bornite; kesterite; ferrokesterite; stannite; electron probe microanalysis; Băița-Bihor skarn deposit

1. Introduction

The Băița-Bihor ore deposit is located in the northwestern part of the Bihor Mountains, Apuseni Mountains, on the upper course of the Crișul Negru river, 3.5 km ENE of Băița village. This deposit together with the Fe skarn deposits at Băișoara (Mașca, Mașca Băișoara, and Cacova) and the Valea Lita Pb-Zn-Cu vein deposit are the northernmost ore occurrences in the Banatitic Magmatic and Metallogenic Belt (BMMB). Băița-Bihor is the most significant ore deposit in the North Apuseni Mountains (NA) [1] (Figure 1a). Băița-Bihor is a polymetallic skarn deposit consisting of tens of individual orebodies which can be considered altogether as distal to the fluid source, i.e., a granite to granodiorite-diorite at depth. At the ore deposit scale, however, there is clear zonation in terms of metals, whereby Mo-Bi-Cu-W, Cu-W, and Pb-Zn-B skarn ores are placed proximal to distal relative to the inferred intrusive fluid source.

The abundance of Bi-sulfosalts (e.g., wittichenite, emplectite, cosalite, lillianite, hodrushite, bismuthinite, aikinite, etc.) in the Băița-Bihor ores was previously noticed by several authors [2–6]. Tin minerals have not, however, been identified in prior studies, even if the existence of a tin geochemical anomaly was reported by many authors [3,7–10].

With a presumed starting point of mining activity during the Roman Dacia period (2nd–3rd c. AD) [11], over 120 mineral species have been described from Băița-Bihor [12]. Băița-Bihor is the type locality of seven minerals, i.e., hemimorphite, described in 1853 according to Papp [13], szaibelyite [14], padăraite [15], makovickyite [16], cuproneite [17], and grațianite [18]. The present contribution focuses on Bi- and Sn- minerals from two orebodies located in a relatively proximal position relative to the fluid source, i.e., Blidar Contact and Antoniu breccia pipe and its Antoniu North branch.

2. Geological Background

The BMMB belt, also known as the Upper Cretaceous Apuseni-Banat-Timok-Srednogorie (ABTS) belt [19,20], evolved in a back-arc setting related to the subduction of the Neotethys [1,20,21]. This belt hosts more than 50 ore deposits of various genetic types, e.g., porphyry, epithermal, skarn, veins [22,23], which have been mined throughout history for several commodities, i.e., Cu, Au, Mo, Pb, Zn, Fe ± Bi, U, Ti, Co, Ni, B [23].

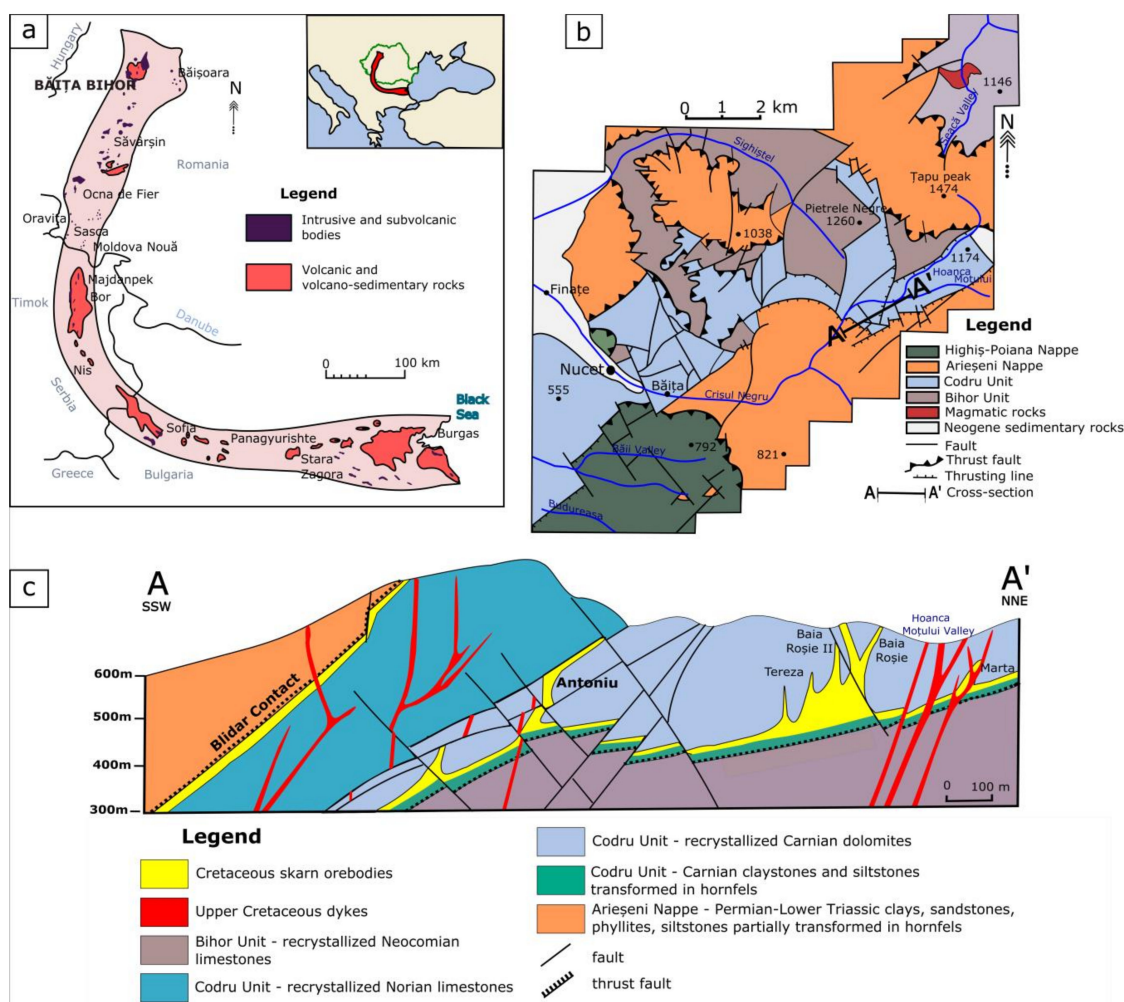


Figure 1. The location and geology of the Băița-Bihor ore deposit. (a) The extent of the Banatitic Magmatic and Metallogenetic Belt in SE Europe and the location of Băița-Bihor (simplified from Cioflică and Vlad [24]); (b) simplified geology of the Băița-Bihor area [11]; (c) cross-section through the Băița-Bihor ore deposit along cross-section A-A' line indicated on (b) showing the location of the main orebodies [11].

The geological structure of the Băița-Bihor area reflects the tectonic structure of the Northern Apuseni Mountains. The Bihor Unit forms a basement that is unconformably overlain by several nappes that belong to the Codru nappe system and the Biharia nappe system [11,25,26] (Figure 1b,c).

The Bihor Unit consists of Jurassic - Lower Cretaceous detritic and calcareous formations. The overlying Codru nappe system is built up of the Codru unit, which is composed of several nappes (Bătrânescu, Următ, and Vetre) covered by the Arieșeni nappe [27,28]. The Codru unit comprises a complete Triassic sequence composed of sandstones, limestones, and dolomites and is unconformably overlain by Permian (Early Carboniferous?)—Lower Triassic detritic sedimentary rocks of the Arieșeni nappe [29]. The entire nappe system was subsequently pierced by Late Cretaceous magmatism [1,30],

represented by a deep-seated granite to granodiorite-diorite batholith accompanied by subvertical basic to intermediate composition dykes.

The metasomatic products (i.e., calcic, magnesian, and calcic-magnesian skarns) are located mainly in the Codru Unit [8,26,31] and formed upon the contact of different lithologies along the main tectonic structures, e.g., thrust planes, faults intersection or major faults (Figure 1c). These discontinuities channeled hot mineralizing fluids up to 1.5 km away from the pluton [11,25,26] and controlled the genesis of skarn deposits with a clear W to E lateral zonation [25], i.e., i) Mo (-Bi, Cu, W) deep-proximal zone; ii) Cu (-Bi, W) proximal zone; and iii) Pb-Zn distal zone. Individual orebodies mostly consist of vertical pipe-like structures located at fault intersection zones, i.e., Antoniu, Baia Roşie, Pregna, etc., and tabular orebodies located along the thrust zones, i.e., the Blidar Contact [8,11] (Figure 1c).

Presently exhausted, exploitation of the Blidar Contact orebody started during the Middle Age [11,24,32] and continued on strike over 600 m [11]. This orebody has a tabular morphology with an NW–SE strike and a 45–50° dip towards SW, similar to the Blidar thrust fault [11,32,33] (Figure 1c). The Blidar Contact orebody hosts the most important Mo-Bi concentration within the Băiţa-Bihor deposit [33] and is associated with garnet-wollastonite skarn in the inner part of the orebody, and diopside-garnet-wollastonite skarns in the outer zone [11,33,34]. At the orebody-scale, there is a metal vertical zonation with Bi enrichment in the upper zone, and a horizontal zonation with an inner Mo-Bi zone and an outer Cu-W (-Mo-Bi) zone [11,32,34].

The exploitation of the Antoniu orebody began in the 19th century. This orebody is located in the western part of the deposit. It has a columnar morphology and occurs at the intersection of two major structures striking N60 and N300-310, respectively [11]. It is considered by Cook and Ciobanu [35] to be one of the most important orebodies from the entire Băiţa-Bihor deposit thanks to its dimensions, with a known mined-out vertical section of over 400 m from below the underground level 224 ASL to approximately 650 m ASL. Exploration programs executed so far have not intercepted the lower limit of the orebody.

The high-grade Cu(-Bi-W-B) ores of the Antoniu orebody [11,34] suggests a proximal position relative to the fluid source [36–38]. Skarn assemblages within the Antoniu ore pipe vary from diopside(±grandite)-bearing skarns in the inner zone to wollastonite/vesuvianite-humite-bearing skarns in the outer zones [8,11]. The formation of the Antoniu orebody has been accompanied by dedolomitisation, which formed an external halo marking the transition to the dolomite host rocks [8,11]. The orebody displays zonation in terms of metals with Cu enrichment in the upper part, Bi enrichment in the lower part, altogether with Pb-Zn [37,38], and B-bearing minerals in the peripheral zone [11,34,39–42]. The Antoniu orebody has a northern apophysis (Figure 1c) that lies approximately 300 m north, known as Antoniu North [3,35]. The discovery and mining of Antoniu North started in 2002 and ceased in 2013. Underground mining is planned to resume during 2020. The morphology of the ore body is still poorly known in detail but seems to possess an irregular breccia dyke morphology, possibly merging with the Antoniu orebody at depth.

3. Materials and Methods

The studied material consists of ore samples collected from the lowermost central-western part of the Antoniu North orebody (Figure 2a) and the lowermost western part of the Antoniu orebody (Figure 2b–e). The deepest part of these orebodies is nowadays accessible by the underground mining works of level XVIII (224 m ASL), Băiţa mine. Other samples (e.g., Figure 2f) were selected from the “Valeriu Lucca” Ore Deposit Collection, Department of Geology, Babeş-Bolyai University, Cluj-Napoca. These samples were collected in 1971 from the underground works along the so-called Blidar Contact orebody by Professor Ioan Mârza.

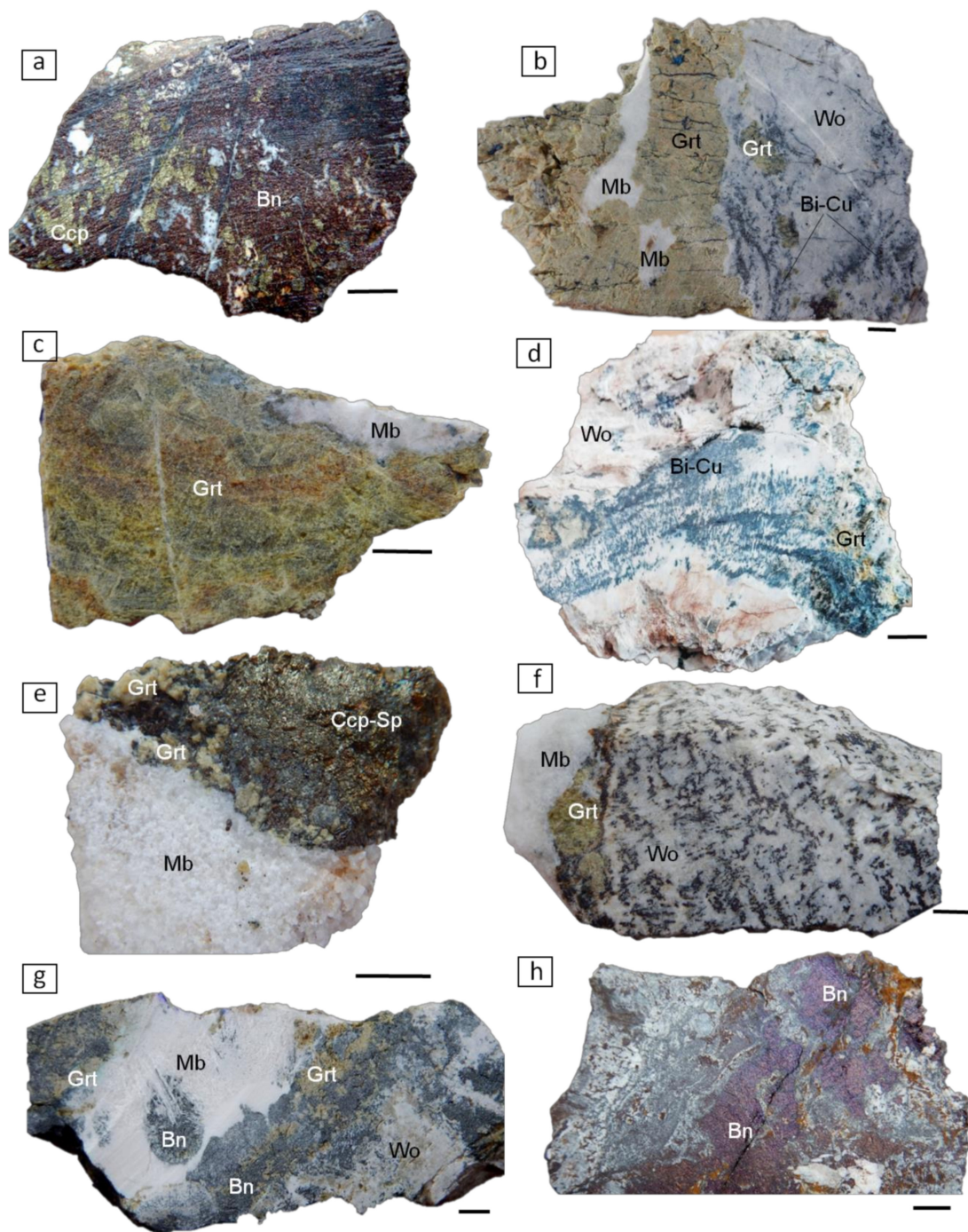


Figure 2. Representative samples from the Antoniu (a—4661), Antoniu North (b—4662, c—4667, d—4669; e—4670, f—5093, g—5094) and Blidar Contact orebodies (h—5095); (a) massive bornite-chalcopyrite ore (4661); (b) grandite skarn with relict marble (left) and wollastonite skarn with Bi-Cu minerals and garnet fragments (right) (4662); (c) grandite skarn with relict marble (4667); (d) wollastonite skarn with Bi-Cu mineralization and garnet fragments (4669); (e) sphalerite-chalcopyrite mineralization, garnet relict, and marble (4670); (f) wollastonite skarn bearing bornite; garnets occur between wollastonite skarn and marble (5093); (g) grandite-wollastonite skarn with bornite and relict marble (5094); (h) massive bornite-chalcopyrite ore (5095). Scale bar: 1 cm. Abbreviations: Bi-Cu: bornite-wittichenite dominant; Bn: bornite; Ccp: chalcopyrite; Sp: sphalerite; Grt: garnet; Mb: marble; Wo: wollastonite.

Optical microscopy, in both transmitted and reflected light, was carried out using a Nikon Eclipse LV100N POL diascopic/episcopic illumination polarizing microscope in the GET Laboratory (Géosciences Environnement Toulouse—Observatoire Midi-Pyrénées), Toulouse, France.

Semi-quantitative chemical data and back-scattered electron (BSE) images were obtained for samples from the Antoniu North and Blidar Contact orebodies using a JSM-6360 scanning electron microscope operated at 20 kV (GET Laboratory) as a preliminary step prior to quantitative electron probe microanalysis. Quantitative chemical analysis of samples from the Blidar Contact orebody was carried out at the UMS 3623—Centre de MicroCaractérisation Raimond Castaing, Toulouse University, France with a CAMECA SXFive electron microprobe using an acceleration voltage of 25 keV, and a beam current of 20 nA. Analytical conditions are presented in Supplementary Table S1. Only those EPMA data with totals between 97.77 and 101.50 (in wt%) were used for subsequent interpretation.

4. Results

4.1. Ore Petrography

4.1.1. The Antoniu and Antoniu North Orebodies

Ores from the Antoniu and Antoniu North orebodies are bornite-dominant. At the microscopic scale, bornite fills open spaces among the skarn minerals (Figure 3a) and creates an ore mineral matrix for the other ore minerals. Part of the bornite formed as a replacement of chalcopyrite (Figure 3b). Additionally, bornite shows partial replacement by digenite (Figure 3a–e).

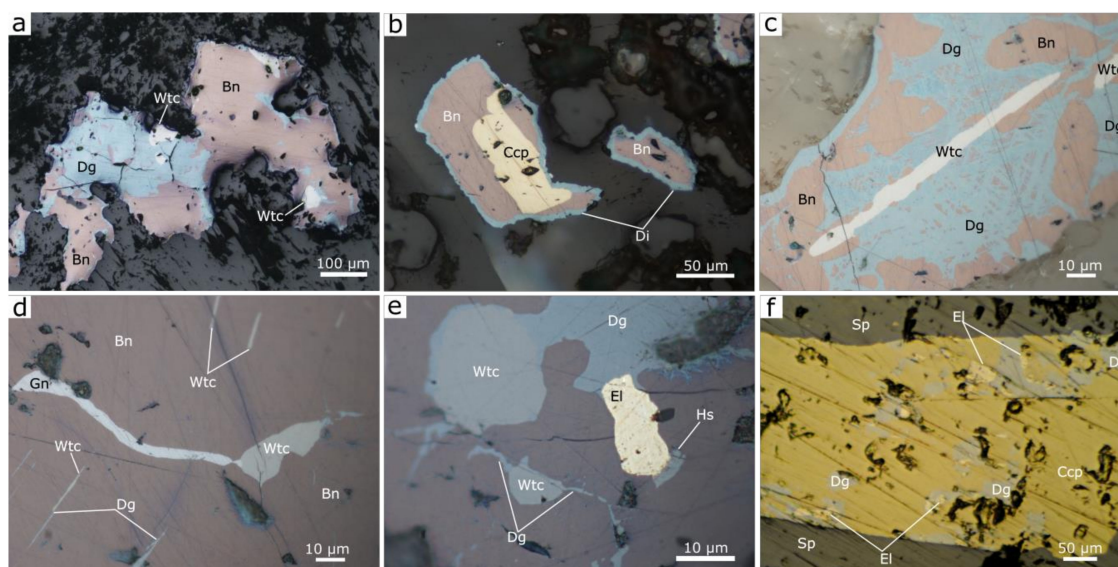


Figure 3. Photomicrographs in the plane-polarized reflected light of Cu-Au-Bi ore from the Antoniu and Antoniu North orebodies; (a) bornite, digenite, and subordinate wittichenite filling spaces among skarn minerals; (b) chalcopyrite grains partly replaced by bornite with digenite rims; (c) wittichenite hosted by bornite displaying network-like replacement by digenite; (d) galena, wittichenite and digenite hosted by bornite; (e) electrum associated with hessite, digenite, and wittichenite hosted by bornite; (f) electrum grains associated with digenite hosted by chalcopyrite. Abbreviations: Bn: bornite, Ccp: chalcopyrite, Dg: digenite, El: electrum, Gn: galena, Hs: hessite, Sp: sphalerite, Wtc: wittichenite.

Wittichenite is frequently observed within bornite and occurs as grains, irregular patches, or filaments of various sizes that range from 10 to maximum 270 μm (Figure 3a,c–e). It was also observed as fine bleb-like exsolutions in bornite or as elongate grains apparently oriented along the main crystallographic axes of the host mineral.

Electrum occurs in Antoniu North orebody as grains of up to 15 μm in size hosted by bornite and intimately related to hessite (Figure 3e). Electrum was also observed as small grains of up to 5 μm included in chalcopyrite hosted by sphalerite (Figure 3f).

Galena occurs as small discontinuous rims of less than 50 μm in length along the margins of coarse bornite grains, and as elongated inclusions hosted by bornite (Figure 3d).

Digenite is quite abundant in the studied samples and occurs as a late replacement product of bornite and chalcopyrite (Figure 3a–c). Digenite occurs as rims, irregular replacement blebs, and veinlets within bornite, usually fissure- or void-controlled, or as regular network-like inclusions (Figure 3c). Digenite shows minor replacement by covellite showing a “dusty” texture with very small grains.

4.1.2. The Blidar Contact Orebody

Bornite and associated ore minerals occur as massive pods exceeding several centimeters across, as smaller nests composed of grains dispersed among skarn minerals, or as irregular veinlets. Bornite grains show common replacement by digenite along grain boundaries or crosscutting fissures. Digenite is locally replaced by covellite, which also replaces bornite (Figure 4a).

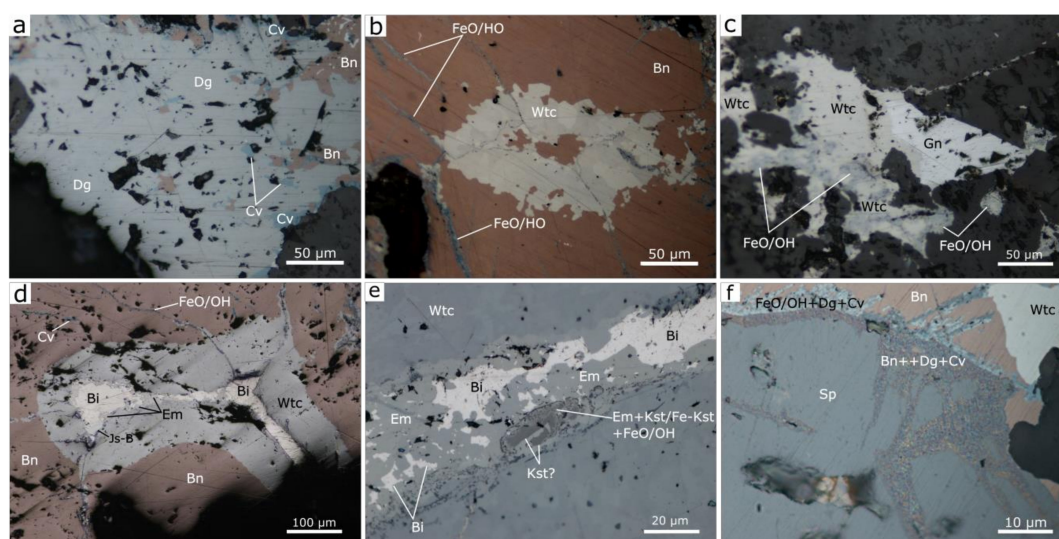


Figure 4. Photomicrographs in plane-polarized reflected light of Cu-Bi-Sn ore from the Blidar Contact orebody; (a) bornite replaced by digenite and covellite; (b) wittichenite nest hosted by bornite; (c) wittichenite-galena assemblage with partial replacement of wittichenite by Fe-oxides/hydroxides; (d) native bismuth filling a vug within bornite associated with emplectite and jos ite-B and a well-developed border of wittichenite; (e) irregular grains of k sterite(?) surrounded by emplectite and a mixture phase; (f) detail of bornite-sphalerite contact. Abbreviations: Bi: native bismuth, Bn: bornite, Cv: covellite, Dg: digenite, Em: emplectite, FeO/OH: Fe oxides/hydroxides, Gn: galena, Js-B: jos ite-B, Kst (?): possible k sterite, Sp: sphalerite, Wtc: wittichenite.

Wittichenite occurs as small worm-like intergrowth within bornite, small blebs, and grain aggregates of up to 200 μm across (Figure 4b). It also occurs as up to 150 \times 100 μm -sized grains associated with galena (Figure 4c). Wittichenite is intergrown with bornite and contains bornite, digenite, and bornite-digenite blebs or irregular patches.

Galena occurs as inclusions in bornite, sphalerite, and in covellite replacing bornite/digenite. Galena is locally corroded by wittichenite (Figure 4c) or by Fe-oxides/hydroxides.

Native bismuth, jos ite-B, and emplectite are associated with wittichenite hosted by bornite (Figure 4d). The occurrence of native bismuth is controlled by the presence of voids, cracks, and microfractures (Figure 4d,e).

Joséite-B occurs as sub-rounded and irregular grains up to 95 μm at contacts between wittichenite with native bismuth (Figure 4d) and as irregular inclusions of up to 50 μm hosted by bornite. When hosted by bornite, Joséite-B is often associated with wittichenite.

Emplectite appears as a continuous border around native bismuth, along mutual grain boundaries between Joséite-B and wittichenite (Figure 4d,e), as irregular inclusions within the bornite associated with the native bismuth, and as elongate grains in contact with Sn-bearing minerals. The contact between wittichenite and emplectite is frequently marked by Fe oxides/hydroxides. The presence of native bismuth inclusions within emplectite (Figure 4e) indicates that native bismuth was partly replaced by emplectite.

Sphalerite is common within the ore. It was observed mostly as inclusions ranging in size from 70 to 300 μm , hosted by bornite. The contact zone between sphalerite and bornite is marked by a reaction zone composed of two sequences: (i) one formed on sphalerite, which contains small-sized sphalerite blebs surrounded by bornite and minor amounts of digenite and covellite, which also advances within sphalerite; and (ii) one formed on bornite which consists of Fe-oxides/hydroxides and digenite associated with minor covellite (Figure 4f). This reaction zone also formed along the sphalerite border even if the bornite-sphalerite contact is sealed by galena or wittichenite, with Fe-oxides/hydroxides concentrated in the adjacent bornite and bornite-sphalerite composite sequence in contact with wittichenite.

Kësterite and ferrokësterite were observed in association with sphalerite, bornite, emplectite, wittichenite, digenite, covellite, and Fe-oxides/hydroxides. These Sn-minerals occur as rounded or irregular grains up to 30 μm hosted by bornite. These two Sn-minerals are difficult to distinguish by optical microscopy alone. The sphalerite-kësterite/ferrokësterite contact is smooth, with no sign of replacement. Kësterite/ferrokësterite grains can display rims of galena that likely indicate the primary boundary of the Sn-minerals. Irregular grain boundaries between bornite and kësterite/ferrokësterite suggest that the kësterite/ferrokësterite grains were not formed in equilibrium with bornite, which partly replaced the outward portion of the Sn-mineral grains.

Stannite occurs as small irregular inclusions (up to 10 μm) within bornite in association with sphalerite and Fe-oxides/hydroxides.

Kësterite(?) associated with native bismuth and related Bi-minerals shows an elongated morphology, with a maximum of 30 μm in length (Figure 4e), concentrated at emplectite-wittichenite grain boundaries.

The BSE images confirm the presence of electrum in Antoniu North orebody (Figure 5a). Additionally, the presence of emplectite, Joséite-B, and native bismuth was confirmed in the Blidar Contact ore (Figure 5b,c) with native bismuth inclusions in wittichenite and relict grains within emplectite and Joséite-B. The BSE images also revealed the formation of Fe-oxides/hydroxides and digenite within bornite along the contact with sphalerite (Figure 5d).

The existence of the Sn-minerals in Blidar Contact orebody, likely kësterite(?), and a mixture of secondary phases containing Cu, Sn, S, Fe, Bi, O have been also confirmed (Figure 5e). Clear replacement relationships exist among these minerals as suggested among others by the presence of relict Sn-sulfide grains within emplectite (black spots).

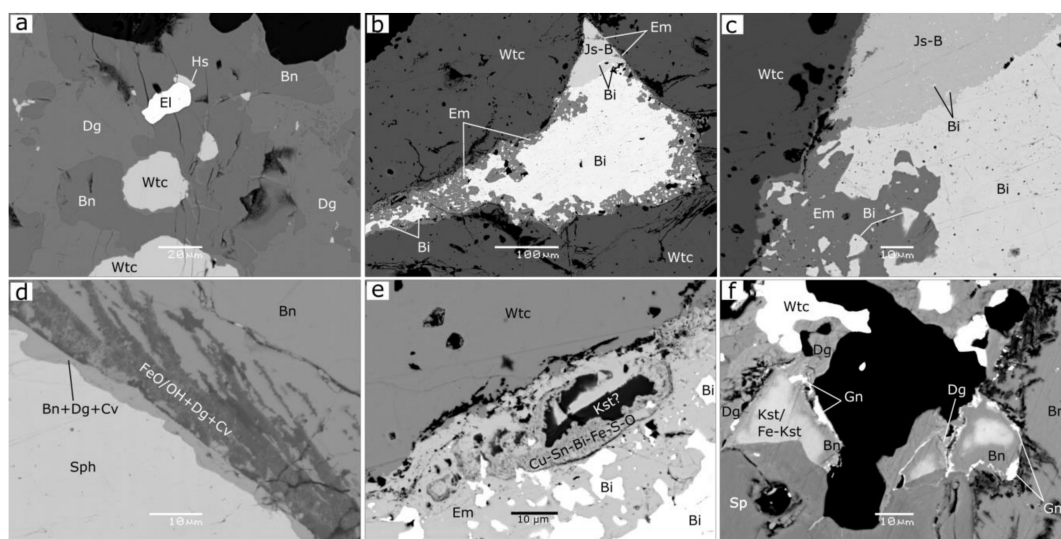


Figure 5. SEM-BSE images for electrum, Bi-, Zn- and Sn- minerals from the Antoniu North (a) and Blidar Contact orebodies (b–f); (a) electrum associated with hessite and digenite; (b) the void within wittichenite filled with native bismuth, emplectite, and joséite-B; (c) detail of (b) with native bismuth relicts hosted by emplectite and joséite-B; (d) bornite-sphalerite contact; (e) k esterite(?) and a mixture of secondary phases in association with emplectite at the native bismuth-wittichenite contact; (f) k esterite/ferrok esterite with galena rims associated with bornite, digenite, sphalerite, and wittichenite (from Andrii and T amaş [9], with permission from the editor). Abbreviations: Bi: native bismuth; Bn: bornite; Cv: covellite; Dg: digenite; El: electrum; Em: emplectite; FeO/OH: Fe oxides/hydroxides; Js-B: jos eite-B; Kst?: possibly k esterite; Kst: k esterite; Fe-Kst: ferrok esterite; Sp: sphalerite; Wtc: wittichenite; Cu-Sn-Bi-Fe-S-O: the mixture of secondary mineral phases.

4.2. Crystal Chemistry

EPMA data for bornite are listed in Table 1 and confirm a wide chemical variation range for the analyzed elements, likely related to the presence of associated and included ore minerals. Sphalerite, identified based on its optical properties, was confirmed by EPMA data on samples from the Blidar Contact orebody (Table 1). Quantitative EPMA data for bismuth minerals (Tables 2 and 3) are in agreement with the previously acquired semi-quantitative SEM-EDS chemical data and optical microscopy interpretation and confirm the occurrence of native bismuth, wittichenite, emplectite, and jos eite-B.

EPMA data for Sn-minerals (Table 4) indicate the presence of k esterite, ferrok esterite, and stannite within the Blidar Contact orebody.

Table 1. Quantitative chemical data (wt%) for bornite and sphalerite from the Blidar Contact orebody.

Mineral (Analyses/Grains)		Element (wt%) *								Calculated Formula	
		S	Ag	Fe	Cu	Zn	Mn	Cd	Sn		Total
		(based on 10 apfu)									
1	bornite (6/3)	26.32	bdl	11.47	62.61	bdl	bdl	bdl	0.47	100.87	$(\text{Cu}_{4.89}, \text{Sn}_{0.02})_{\Sigma} = 4.91 \text{Fe}_{1.02} \text{S}_{4.07}$
2		26.16	0.27	10.84	63.37	bdl	bdl	bdl	bdl	100.64	$(\text{Cu}_{4.96}, \text{Ag}_{0.01})_{\Sigma} = 4.97 \text{Fe}_{0.97} \text{S}_{4.06}$
3		26.69	0.24	11.49	62.77	bdl	bdl	bdl	0.10	101.29	$(\text{Cu}_{4.87}, \text{Ag}_{0.01}, \text{Sn}_{0.004})_{\Sigma} = 4.88 \text{Fe}_{1.01} \text{S}_{4.10}$
4		26.64	0.31	10.13	58.14	1.12	bdl	0.07	2.83	99.24	$(\text{Cu}_{4.64}, \text{Sn}_{0.12}, \text{Ag}_{0.02})_{\Sigma} = 4.78 (\text{Fe}_{0.92}, \text{Zn}_{0.09}, \text{Cd}_{0.003})_{\Sigma} = 1.01 \text{S}_{4.21}$
5		27.18	bdl	8.96	49.39	3.16	bdl	0.12	9.80	98.62	$(\text{Cu}_{4.05}, \text{Sn}_{0.43})_{\Sigma} = 4.48 (\text{Fe}_{0.84}, \text{Zn}_{0.25}, \text{Cd}_{0.006})_{\Sigma} = 1.10 \text{S}_{4.42}$
6		26.10	0.79	3.02	69.70	0.43	bdl	bdl	0.23	100.27	$(\text{Cu}_{5.54}, \text{Sn}_{0.01})_{\Sigma} = 5.55 (\text{Fe}_{0.27}, \text{Zn}_{0.03})_{\Sigma} = 0.30 \text{S}_{4.11}$
		(based on 2 apfu)									
7	sphalerite (3/1)	32.99	bdl	5.23	7.37	52.02	0.50	0.70	0.13	98.94	$(\text{Zn}_{0.78}, \text{Cu}_{0.11}, \text{Fe}_{0.09}, \text{Mn}_{0.009}, \text{Cd}_{0.006}, \text{Sn}_{0.001})_{\Sigma} = 1.00 \text{S}_{1.00}$
8		32.80	bdl	7.05	3.20	52.32	1.74	1.04	bdl	98.15	$(\text{Zn}_{0.79}, \text{Fe}_{0.12}, \text{Cu}_{0.05}, \text{Mn}_{0.03}, \text{Cd}_{0.009})_{\Sigma} = 1.00 \text{S}_{1.00}$
9		32.28	bdl	4.37	10.42	50.04	0.29	0.73	0.87	99.00	$(\text{Zn}_{0.75}, \text{Cu}_{0.16}, \text{Fe}_{0.08}, \text{Mn}_{0.005}, \text{Sn}_{0.007}, \text{Cd}_{0.006})_{\Sigma} = 1.01 \text{S}_{0.99}$

* Below detection limit values were obtained for As, Pb, Sb, Bi in all measured points; additionally, below detection limit values were obtained for Te and Se for the bornite point analyses from row 3. "bdl" = below detection limit.

Table 2. Quantitative chemical data (wt%) for native bismuth, wittichenite, and emplectite from the Blidar Contact orebody.

Mineral (Analyses/Grains)		Element (wt%) *							Calculated Formula	
		S	Ag	Fe	Cu	Sb	Bi	Sn		Total
		(based on 1 apfu)								
1	native bismuth (5/2)	bdl	bdl	bdl	bdl	0.09	98.04	bdl	98.13	$(\text{Bi}_{1.00}, \text{Sb}_{0.002})_{\Sigma} = 1.00$
2		bdl	bdl	bdl	bdl	bdl	98.38s	bdl	98.38	$\text{Bi}_{1.00}$
3		bdl	bdl	bdl	bdl	bdl	99.88	bdl	99.88	$\text{Bi}_{1.00}$
4		bdl	bdl	bdl	0.34	bdl	98.03	bdl	98.03	$(\text{Bi}_{0.99}, \text{Cu}_{0.01})_{\Sigma} = 1.00$
5		bdl	bdl	bdl	bdl	bdl	99.29	bdl	99.29	$\text{Bi}_{1.00}$
		(based on 7 apfu)								
6	wittichenite (9/3)	19.82	0.24	0.12	38.65	bdl	41.63	bdl	100.46	$(\text{Cu}_{2.97}, \text{Ag}_{0.01}, \text{Fe}_{0.01})_{\Sigma} = 2.99 \text{Bi}_{0.98} \text{S}_{3.03}$
7		19.73	0.31	0.06	38.50	bdl	41.80	bdl	100.40	$(\text{Cu}_{2.97}, \text{Ag}_{0.01}, \text{Fe}_{0.005})_{\Sigma} = 2.99 \text{Bi}_{0.98} \text{S}_{3.02}$
8		19.70	0.47	0.12	38.55	bdl	40.73	bdl	99.57	$(\text{Cu}_{2.99}, \text{Ag}_{0.02}, \text{Fe}_{0.01})_{\Sigma} = 3.00 \text{Bi}_{0.96} \text{S}_{3.02}$
9		19.82	0.22	0.04	38.23	bdl	40.64	bdl	98.95	$(\text{Cu}_{2.97}, \text{Ag}_{0.01}, \text{Fe}_{0.004})_{\Sigma} = 3.00 \text{Bi}_{0.96} \text{S}_{3.05}$
10		19.68	0.34	0.10	38.58	bdl	41.13	bdl	99.83	$(\text{Cu}_{2.99}, \text{Ag}_{0.02}, \text{Fe}_{0.009})_{\Sigma} = 3.02 \text{Bi}_{0.97} \text{S}_{3.01}$
11		20.02	0.27	0.09	38.59	bdl	40.62	bdl	99.59	$(\text{Cu}_{2.97}, \text{Ag}_{0.01}, \text{Fe}_{0.008})_{\Sigma} = 2.99 \text{Bi}_{0.95} \text{S}_{3.06}$
12		19.45	bdl	0.22	38.19	bdl	41.16	bdl	99.02	$(\text{Cu}_{2.98}, \text{Ag}_{0.007}, \text{Fe}_{0.02})_{\Sigma} = 3.01 \text{Bi}_{0.98} \text{S}_{3.01}$
13		19.17	0.22	0.40	37.82	bdl	41.79	bdl	99.40	$(\text{Cu}_{2.97}, \text{Ag}_{0.01}, \text{Fe}_{0.04})_{\Sigma} = 3.02 \text{Bi}_{1.00} \text{S}_{2.98}$
14		19.97	0.24	bdl	37.90	bdl	40.16	0.23	98.50	$(\text{Cu}_{2.95}, \text{Ag}_{0.01}, \text{Sn}_{0.01})_{\Sigma} = 2.99 \text{Bi}_{0.95} \text{S}_{3.08}$
		(based on 4 apfu)								
15	emplectite (4/4)	19.85	bdl	bdl	18.56	bdl	60.20	bdl	98.61	$\text{Cu}_{0.97} \text{Bi}_{0.96} \text{S}_{2.06}$
16		19.70	bdl	0.12	18.34	bdl	59.62	bdl	97.78	$(\text{Cu}_{0.97}, \text{Fe}_{0.007})_{\Sigma} = 0.98 \text{Bi}_{0.96} \text{S}_{2.07}$
17		19.59	bdl	bdl	18.18	bdl	60.45	bdl	98.22	$(\text{Cu}_{0.97}, \text{Fe}_{0.002})_{\Sigma} = 0.97 \text{Bi}_{0.96} \text{S}_{2.06}$
18		20.12	bdl	bdl	18.32	bdl	59.35	bdl	97.79	$\text{Cu}_{0.96} \text{Bi}_{0.95} \text{S}_{2.09}$

* Below detection limit values were obtained for As, Pb, Mn, Zn, Cd, in all measured points; additionally, below detection limit values were obtained for Te and Se for the native bismuth and emplectite. "bdl" = below detection limit.

Table 3. Quantitative chemical data (wt%) for joséite-B from the Blidar Contact orebody.

Mineral (Analyses/Grains)	Element (wt%) *							Calculated Formula	
	S	Fe	Cu	Sb	Bi	Te	Se		Total
									(based on 7 apfu)
1	2.85	bdl	bdl	0.13	72.85	22.18	bdl	98.01	$(\text{Bi}_{3.98}, \text{Sb}_{0.01})_{\Sigma} = 3.99 \text{Te}_{1.99} \text{S}_{1.02}$
2	2.82	bdl	0.14	0.14	72.30	22.43	bdl	97.83	$(\text{Bi}_{3.95}, \text{Cu}_{0.03}, \text{Sb}_{0.01})_{\Sigma} = 3.96 \text{Te}_{2.01} \text{S}_{1.00}$
3	2.91	bdl	bdl	0.16	73.40	21.30	bdl	97.77	$(\text{Bi}_{4.03}, \text{Sb}_{0.02})_{\Sigma} = 4.05 \text{Te}_{1.91} \text{S}_{1.04}$
4	2.77	bdl	0.13	0.11	73.91	22.30	bdl	99.22	$(\text{Bi}_{4.01}, \text{Cu}_{0.02}, \text{Sb}_{0.01})_{\Sigma} = 4.04 \text{Te}_{1.98} \text{S}_{0.98}$
5	2.77	0.13	0.50	0.12	72.40	22.62	bdl	98.54	$(\text{Bi}_{3.90}, \text{Cu}_{0.09}, \text{Fe}_{0.03}, \text{Sb}_{0.01})_{\Sigma} = 4.03 \text{Te}_{2.00} \text{S}_{0.97}$
6	2.99	bdl	0.21	0.10	73.00	22.23	bdl	98.53	$(\text{Bi}_{3.94}, \text{Cu}_{0.04}, \text{Sb}_{0.009})_{\Sigma} = 3.99 \text{Te}_{1.96} \text{S}_{1.05}$
7	2.80	0.07	0.37	0.15	71.84	22.68	bdl	97.91	$(\text{Bi}_{3.90}, \text{Cu}_{0.07}, \text{Fe}_{0.01}, \text{Sb}_{0.01})_{\Sigma} = 3.99 \text{Te}_{2.02} \text{S}_{0.99}$
8	2.86	bdl	0.14	0.17	73.76	22.84	bdl	99.77	$(\text{Bi}_{3.95}, \text{Cu}_{0.02}, \text{Sb}_{0.02})_{\Sigma} = 3.99 \text{Te}_{2.01} \text{S}_{2.00}$
9	2.65	bdl	0.26	0.17	75.47	20.69	bdl	99.24	$(\text{Bi}_{4.13}, \text{Cu}_{0.05}, \text{Sb}_{0.02})_{\Sigma} = 4.20 \text{Te}_{1.85} \text{S}_{0.95}$
10	2.97	bdl	0.18	0.14	72.77	22.38	0.13	98.57	$(\text{Bi}_{3.92}, \text{Cu}_{0.03}, \text{Sb}_{0.01})_{\Sigma} = 3.96 \text{Te}_{1.98} (\text{S}_{1.04}, \text{Se}_{0.02})_{\Sigma} = 1.06$
11	2.88	0.11	0.44	0.13	73.45	22.22	0.21	99.44	$(\text{Bi}_{3.92}, \text{Cu}_{0.08}, \text{Fe}_{0.02}, \text{Sb}_{0.01})_{\Sigma} = 4.03 \text{Te}_{1.94} (\text{S}_{1.00}, \text{Se}_{0.03})_{\Sigma} = 1.03$
12	2.99	bdl	0.11	0.12	72.90	21.97	0.37	98.46	$(\text{Bi}_{3.93}, \text{Cu}_{0.02}, \text{Sb}_{0.01})_{\Sigma} = 3.96 \text{Te}_{1.94} (\text{S}_{1.05}, \text{Se}_{0.05})_{\Sigma} = 1.10$
13	2.83	bdl	0.49	0.13	73.13	21.88	0.81	99.27	$(\text{Bi}_{3.90}, \text{Cu}_{0.09}, \text{Sb}_{0.01})_{\Sigma} = 4.00 \text{Te}_{1.91} (\text{S}_{0.98}, \text{Se}_{0.11})_{\Sigma} = 1.09$
14	2.90	bdl	0.09	0.12	73.15	22.27	0.17	98.70	$(\text{Bi}_{3.96}, \text{Cu}_{0.02}, \text{Sb}_{0.01})_{\Sigma} = 3.98 \text{Te}_{1.97} (\text{S}_{1.02}, \text{Se}_{0.02})_{\Sigma} = 1.04$
15	2.94	bdl	0.19	0.11	72.16	22.52	bdl	97.92	$(\text{Bi}_{3.92}, \text{Cu}_{0.03}, \text{Sb}_{0.01})_{\Sigma} = 3.96 \text{Te}_{2.00} \text{S}_{1.04}$

* Below detection limit values were obtained for As, Ag, Pb, Zn, Mn, Cd, Sn in all measured points. "bdl" = below detection limit.

Table 4. Quantitative chemical data (wt%) for k esterite, ferrok esterite, and stannite from the Blidar Contact ore body.

Mineral (Analyses/Grains)		Analyzed Chemical Element (wt%) *								Calculated Chemical Formula	
		S	Fe	Cu	Zn	Mn	Cd	Sn	Se		Total
(based on 8 apfu)											
1	k�esterite	29.16	2.68	32.24	11.60	bdl	0.46	25.10	na	101.24	$\text{Cu}_{2.18}(\text{Zn}_{0.76}, \text{Fe}_{0.21}, \text{Cd}_{0.02})_{\Sigma} = 0.99\text{Sn}_{0.91}\text{S}_{3.92}$
2	(5/2)	29.09	3.05	32.61	10.46	bdl	0.75	25.27	na	101.23	$\text{Cu}_{2.21}(\text{Zn}_{0.69}, \text{Fe}_{0.24}, \text{Cd}_{0.03})_{\Sigma} = 0.96\text{Sn}_{0.92}\text{S}_{3.91}$
3		28.84	4.38	35.11	6.25	bdl	1.66	25.06	na	101.30	$\text{Cu}_{2.39}(\text{Zn}_{0.41}, \text{Fe}_{0.34}, \text{Cd}_{0.06})_{\Sigma} = 0.81\text{Sn}_{0.91}\text{S}_{3.89}$
4		28.75	2.82	33.65	11.33	bdl	0.26	23.19	na	100.00	$\text{Cu}_{2.29}(\text{Zn}_{0.75}, \text{Fe}_{0.22}, \text{Cd}_{0.01})_{\Sigma} = 0.98\text{Sn}_{0.85}\text{S}_{3.88}$
5		28.68	3.27	34.85	10.63	bdl	0.25	22.20	na	99.88	$\text{Cu}_{2.37}(\text{Zn}_{0.70}, \text{Fe}_{0.25}, \text{Cd}_{0.01})_{\Sigma} = 0.96\text{Sn}_{0.81}\text{S}_{3.86}$
(based on 8 apfu)											
6	ferrok�esterite	28.92	6.10	33.01	3.38	bdl	3.20	26.73	na	101.34	$\text{Cu}_{2.26}(\text{Fe}_{0.48}, \text{Zn}_{0.23}, \text{Cd}_{0.12})_{\Sigma} = 0.83\text{Sn}_{0.98}\text{S}_{3.93}$
7	(2/1)	28.89	5.45	33.22	4.50	bdl	2.77	26.11	na	100.94	$\text{Cu}_{2.28}(\text{Fe}_{0.43}, \text{Zn}_{0.30}, \text{Cd}_{0.11})_{\Sigma} = 0.84\text{Sn}_{0.96}\text{S}_{3.93}$
(based on 8 apfu)											
8		29.99	9.79	30.78	2.66	0.07	1.93	24.72	0.25	100.19	$\text{Cu}_{2.08}(\text{Fe}_{0.75}, \text{Zn}_{0.17}, \text{Cd}_{0.07}, \text{Mn}_{0.005})_{\Sigma} = 1.00\text{Sn}_{0.89}(\text{S}_{4.01}, \text{Se}_{0.01})_{\Sigma} = 4.02$
9		30.50	10.23	30.53	2.22	0.09	0.85	24.86	0.26	99.31	$\text{Cu}_{2.05}(\text{Fe}_{0.78}, \text{Zn}_{0.15}, \text{Cd}_{0.03}, \text{Mn}_{0.007})_{\Sigma} = 0.97\text{Sn}_{0.90}(\text{S}_{4.07}, \text{Se}_{0.01})_{\Sigma} = 4.08$
10	stannite	30.05	9.85	30.34	1.85	0.09	1.47	24.75	0.27	98.40	$\text{Cu}_{2.07}(\text{Fe}_{0.77}, \text{Zn}_{0.12}, \text{Cd}_{0.06}, \text{Mn}_{0.007})_{\Sigma} = 0.95\text{Sn}_{0.90}(\text{S}_{4.06}, \text{Se}_{0.01})_{\Sigma} = 4.07$
11	(6/2)	29.98	9.36	30.63	3.13	0.05	2.09	24.07	0.32	99.31	$\text{Cu}_{2.08}(\text{Fe}_{0.72}, \text{Zn}_{0.21}, \text{Cd}_{0.08}, \text{Mn}_{0.004})_{\Sigma} = 1.01\text{Sn}_{0.87}(\text{S}_{4.03}, \text{Se}_{0.02})_{\Sigma} = 4.04$
12		30.20	10.48	30.64	1.87	0.06	1.23	24.19	0.26	98.67	$\text{Cu}_{2.08}(\text{Fe}_{0.81}, \text{Zn}_{0.12}, \text{Cd}_{0.05}, \text{Mn}_{0.005})_{\Sigma} = 0.98\text{Sn}_{0.88}(\text{S}_{4.05}, \text{Se}_{0.01})_{\Sigma} = 4.06$
13		30.21	10.20	30.52	2.10	bdl	1.27	24.28	0.22	98.58	$\text{Cu}_{2.07}(\text{Fe}_{0.79}, \text{Zn}_{0.14}, \text{Cd}_{0.05})_{\Sigma} = 0.98\text{Sn}_{0.88}(\text{S}_{4.06}, \text{Se}_{0.01})_{\Sigma} = 4.07$

* Below detection limit values were obtained for As, Ag, Pb, Sb, Bi in all measured points; additionally, below detection limit values were obtained for Te for stannite. "bdl" = below detection limit; "na" = not analyzed.

5. Discussion

5.1. Bornite

The massive bornite hosting wittichenite and the bornite grains hosted by Bi-Cu sulfides (Table 1, rows 1–3) are close to stoichiometric [43].

The continuous outer bornite border that envelops a Sn-mineral grain (right grain from Figure 5f; Table 1, rows 4–5) has Cu and Fe contents that decrease from the galena rim towards the Sn-mineral, i.e., from 58.14 to 49.39 wt%, and from 10.13 to 8.96 wt%, respectively. In contrast, Sn content increases from the galena rim towards the adjacent Sn-mineral from 2.83 to 9.80 wt%, reflecting the presence of small inclusions of Sn-mineral [3] which increase in abundance towards the Sn-mineral grain.

Bornite adjacent to ferrokösterite-kösterite grain (left grain in Figure 5f; Table 1 row 6) shows relative enrichment in Cu (69.70 wt%) and Ag (0.79 wt%), coupled with a Fe deficit (3.02 wt%), and minor Sn (0.23 wt%). The apparent Cu excess and Fe deficit are likely produced by a sub-solidus element remobilization.

The morphologies of wittichenite and galena inclusions within bornite (Figure 3d,e) suggest the exsolution of Bi and Pb during cooling as the solid solution field in the system Bi-Cu-Fe-S contracts. The formation of these new minerals is frequently controlled by crystallographic directions, microfractures, and voids. The formation of wittichenite hosted by bornite indicates that the bornite was Bi-saturated [44]. However, bornite analyzed from Băița-Bihor shows a Bi content below the detection limit (0.40 wt%).

Bornite from the Antoniu North orebody also occurs as a replacement of chalcopyrite (Figure 3b), e.g., chalcopyrite-bornite grains with a chalcopyrite core and a bornite rim. In the studied samples, the bornite rim is followed by a digenite band. Bornite replacement by digenite and digenite replacement by covellite have been also observed for the Blidar Contact orebody. These texture relationships suggest that late fluids have remobilized copper, giving an overprint after the skarn formation.

5.2. Sphalerite

The analyzed sphalerite has a slightly different composition compared to ideal (in wt%), i.e., Zn 65.30; Fe 2.60; S 32.10 [43]. It shows a Zn deficit (Table 1, rows 7–9), readily explained by $\text{Fe}^{2+} \rightarrow \text{Zn}^{2+}$ substitution [45] with Fe ranging from 4.37 to 7.05 wt% (Table 1, rows 6–8), and thus exceeding the Fe content of sphalerite described for Băița-Bihor, i.e., 0.13 to 1.30 wt% by Cook et al. [46] and showing a narrower variation than the range 0.15 to 10.3 wt% mentioned by George et al. [37]. The Cu content, with values ranging from 3.20 to 10.42 wt% (Table 1, rows 7–9), exceeds the values reported previously for the sphalerite from Băița-Bihor, e.g., 0.2 wt% [46], and 0.6 wt% [37]. The Cu and Fe excess correlates with the presence of chalcopyrite inclusions in sphalerite.

The analyzed sphalerite contains 0.70–1.04 wt% Cd (Table 1, rows 7–9), slightly higher than the values mentioned by Cook et al. [46] and George et al. [37], i.e., 0.22 to 0.78 wt%, and 0.16 to 0.28 wt%, respectively. The presence of Cd is related to the isomorphous substitution of Cd^{2+} for Zn^{2+} [46]. The Mn values are slightly exceeding the content previously reported for the sphalerite from the Băița-Bihor deposit [37,46]. Its presence is due to the $\text{Zn}^{2+} \leftrightarrow \text{Mn}^{2+}$ substitution [46].

EPMA data acquired for sphalerite grains in contact with Sn-minerals reveal Sn values ranging from 0.13 to 0.87 wt% (Table 1, rows 7–9). These values are higher than those reported previously [37,46] which showed smaller Sn concentrations of <5 ppm. Low Sn and Ag contents in sphalerite could be explained according to the substitution $2(\text{Cu}^+, \text{Ag}^+) + \text{Sn}^{4+} \leftrightarrow 3\text{Zn}^{2+}$ [46]. Overall, concentrations of Cu, Fe, Mn, Cd, and Sn in sphalerite range between 13.01 and 15.8 wt%. These values are close to or slightly exceed the maximum amount of minor and trace elements that sphalerite typically hosts [46,47].

5.3. Bi-Cu-Sulfosalts and Bi-Tellurides

EPMA data (Table 2, rows 1–5) confirm the occurrence of native bismuth (98.03 to 99.88 wt% Bi, and traces of Cu and Sb). Wittichenite (Table 2, rows 6–14), emplectite (Table 2, rows 15–18), and joséite-B (Table 3) are close to stoichiometric.

Textural relationships of wittichenite, galena, joséite-B, and native bismuth with bornite suggest Bi and Pb exsolution during the cooling of the ore. The formation of wittichenite, native bismuth, and joséite-B indicates that bornite was Bi-saturated [44] with $\text{Bi:X} > 1$, where $\text{X} = \text{Te, S, Se}$, suggesting the existence of a reducing environment at the time of formation.

Textural relationships observed among the Bi-minerals hosted by bornite from the Blidar Contact orebody and their chemical compositions suggest that native bismuth occurred first within bornite. It was subsequently partially replaced by joséite-B, as evidenced by the existence of native bismuth inclusions within joséite-B. Subsequently, the migration of Cu from bornite towards native bismuth and joséite-B in parallel with the Bi migration from native bismuth and joséite-B towards bornite produced wittichenite on the bornite side and emplectite on the native-bismuth and joséite-B side.

5.4. Cu-Sn-Zn(Fe)-S Minerals

The k esterite-stannite pseudobinary system has been continuously investigated since the 1960s, with a focus on the crystal structure and the chemical composition of the system members [48–58]. Stannite and k esterite are the end-members of the stannite-k esterite join system [48,49,51,52]. The two end-members form separate solid solutions and can be differentiated based on their chemical composition and crystal structure, k esterite being the Zn-dominant end-member crystallizing in the $I\bar{4}$ space group, and stannite the Fe-rich member of the system with the $I\bar{4}2m$ space group [51]. Between the two end members, there is an intermediate phase, namely ferrok esterite [53]. Ferrok esterite is the low-temperature polymorph of stannite [52], having a chemical composition similar to stannite and a crystal structure close to that of k esterite [53]. Therefore, ferrok esterite represents the Fe-rich analog of k esterite, with which it may form a solid solution [53].

Electron probe microanalysis of stannite from different occurrences allowed Springer [48] to point out a significant variation in the metal ratios, with an important Zn enrichment. This author stated that a complete solid solution exists between Fe-pure stannite and Zn-pure k esterite. Later, Springer [49] stated that the k esterite-stannite system is pseudobinary and proposed the first phase diagram for the system. He demonstrated that a complete solid solution exists between the two end-members above 680 °C and a structural change in the stannite structure occurs at 680 °C with the formation of a transition phase. A high- and a low-temperature stannite-k esterite phase consequently formed, being separated by a two-phase region. As the temperature decreases, an increase of zinc in the Fe-Zn site occurs and the composition is enriched in Zn and two stannite phases are formed, a β -high temperature phase, and an α -low-temperature phase. According to Moore and Howie [55], k esterite is isostructural with the β -high temperature phase. If the k esterite-stannite system is cooled in the two-phase region, ferrok esterite-k esterite exsolutions in stannite should appear in stannite.

Kissin and Owens [53] claimed the presence of a miscibility gap between the two end-members of the k esterite-stannite system; however, Corazza et al. [59] and Bernadini et al. [56] proposed the existence of a continuous solid-solution. Petruk [60] stated that the minerals sharing a stannite crystal structure might contain up to 55 at% Zn in the Fe-Zn site, and the minerals with a k esterite crystal structure might contain up to 55 at% Fe in the Fe-Zn site. This author also mentioned ‘ferrian-k esterite’, grouping minerals with a k esterite-like crystal structure, 25–55% Fe in the Fe-Zn site and significant concentrations of indium, and ‘zincian-stannite’, or minerals from the stannite field with a Zn-rich composition, with up to 40–55% Zn in the Fe-Zn sites, the latter also having been described by Springer [49] and Moore and Howie [55]. Zn-rich stannite was also studied from Otoge (Japan) by Watanabe et al. [57], who mentioned that the Zn-rich phase of stannite is characterized by $\text{Fe}/(\text{Fe} + \text{Zn})$ ratios in the 0.49–0.71 range. Kissin and Owens [53] demonstrated that the zincian-stannite described by Moore and Howie [55] is actually ferrok esterite and the ferrian-k esterite is, in fact, petrukite.

A plot of EPMA data acquired on Cu-Sn-Zn(Fe)-S minerals from Băița-Bihor (Table 4) on the Cu/(Cu + Sn) vs. Fe/(Fe + Zn) diagram of Petruk [60] allows for discrimination of the Cu-Sn rich minerals belonging to the stannite group, i.e., k esterite, ferrok esterite and stannite (Figure 6).

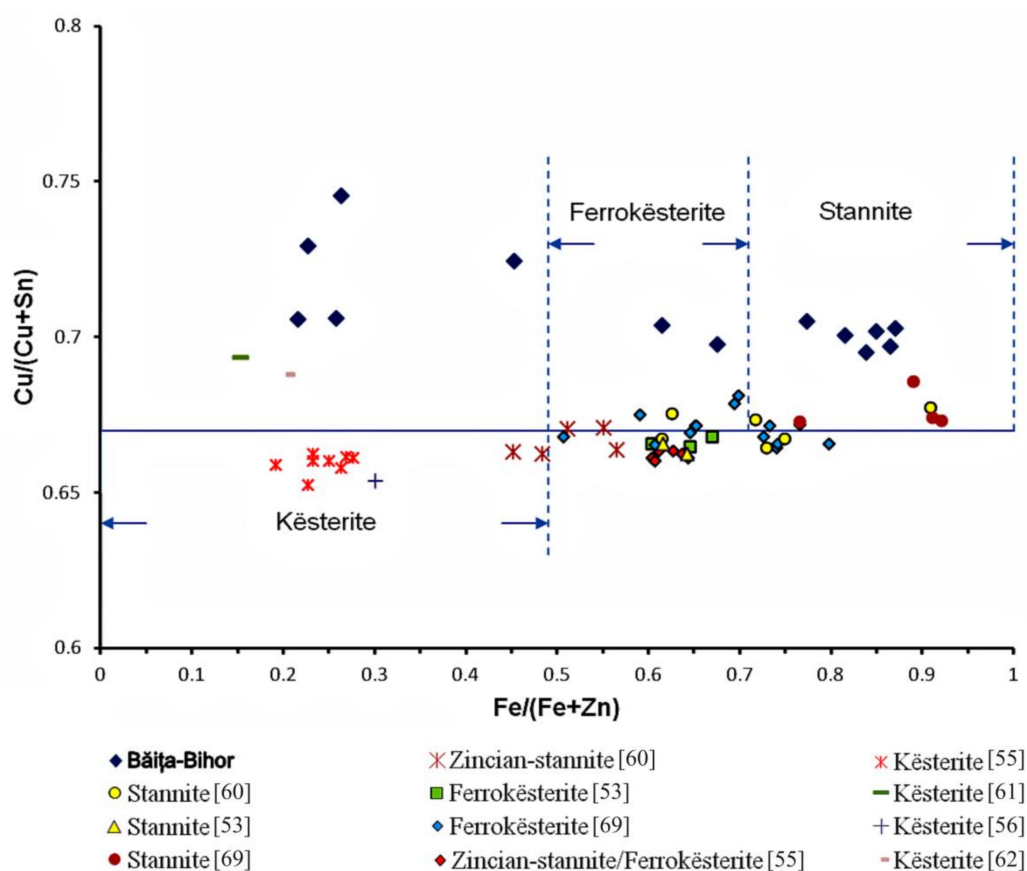


Figure 6. Chemical composition of stannite group minerals shown on a plot of Cu/(Cu + Sn) vs. Fe/(Fe + Zn) after Petruk [60]. Published data from other occurrences are also given. The blue dashed lines separate the approximate stability field of k esterite, ferrok esterite, and stannite based on Fe/(Fe + Zn) ratio according to intervals proposed by Watanabe et al. [57].

The chemical composition of analyzed k esterite from Băița-Bihor is generally close to the standard composition described for the K ester deposit, Russia [61], and to that described from the Panagyurishte ore district, Bulgaria [62]. The Cu/(Cu + Sn) ratios for the k esterite from Băița-Bihor have an average value of 0.72, all greater than the 0.69 value obtained by Ivanov and Pyatenko [61], and by Bogdanov et al. [62].

Cadmium is the single element present at concentrations above the minimum detection limit; a negative correlation is noted between Fe vs. (Zn + Cd). The Fe-rich k esterite occurs in closer association with bornite, whereas Zn-rich k esterite is associated with sphalerite.

EPMA data (Table 4, rows 6–13) and position on the diagram of Cu/(Cu + Sn) vs. Fe/(Fe + Zn) (Figure 6) allows for confirmation of the occurrence of ferrok esterite and k esterite, with ferrok esterite forming the inner part, and k esterite the outer part, of a given grain.

Ferrok esterite has a composition resembling that described from the Cligga mine, England, with the average chemical formula $\text{Cu}_{1.99}(\text{Fe}_{0.67}\text{Zn}_{0.33})_{\Sigma=1.00}\text{Sn}_{0.99}\text{S}_{4.02}$ corresponding to (in wt%) Cu 29.5; Sn 27.4; Fe 8.7; Zn 5.0; S 30.1; Cd 0.1; and Mn 0.1 [53]. Ferrok esterite from Băița-Bihor (Table 4, rows 6–7) has greater values for Cu (33.01–33.22 wt%) and Cd (2.77–3.20 wt%), and smaller average values (in wt%) for Sn (26.42), Zn (3.94), Fe (5.78) and S (28.91) as compared to the composition reported by Kissin and Owens [53].

Iron values generally follow a negative trend with Zn and Cd, suggesting a Fe → (Zn + Cd) substitution (Table 4, rows 6–7). However, the analyzed ferrokësterite remains on the Fe-rich side of the Fe-Zn binary (Figure 6). The average Cu:(Fe,Zn,Cd):Sn ratio 2.27:0.83:0.97 is slightly different from the ideal 2:1:1 ratio [49]. The overall metal/sulfur ratio (including Cd) is 1:0.97, close to the ideal 1:1 [49].

Considering the limit of the ferrokësterite stability field at Fe/(Fe + Zn) = 0.71 [57], all the EPMA points with Fe/(Fe + Zn) ratio values >0.71 are considered here as being stannite, the Fe end-member of the kësterite-stannite system. The possible occurrence of sub-micron stannite inclusions in chalcopyrite and bornite, respectively, in Băița-Bihor was proposed by Cioflică et al. [8] based on geochemical analyses, and later by Cook et al. [3] based on LA-ICP-MS data. The ideal formula of stannite is Cu₂FeSnS₄. However, Springer [48] proposed the formula Cu₂(Fe,Zn)SnS₄ due to large variations in the relative proportions of Zn and Fe. The analyzed stannite is close to the ideal. Aside from Cd (up to 2.09 wt%), Mn (up to 0.09 wt%) and Se (up to 0.32 wt%), the average metal/sulfur ratio 0.99:1.02 remains close to stoichiometric [49]. The (Fe + Mn) values generally follow a negative trend, with (Zn + Cd) suggesting (Fe + Mn) → (Zn + Cd) substitution.

Overall, as shown in Figure 6, all the studied Sn-bearing minerals have higher Cu/(Cu + Sn) ratios compared to the data in the literature, due to a higher Cu content and/or a Sn deficit. Similarly, the chemical composition of the Sn-bearing minerals indicates a wide Fe-Zn substitution, with Fe/(Fe + Zn) ranging from 0.22 to 0.87.

According to Moore and Howie [55] and Nekrasov et al. [63], Sn-minerals associated with sphalerite are typically relatively enriched in Zn. Nekrasov et al. [63] claimed that kësterite-ferrokësterite may form starting from stannite, according to the equation Cu₂FeSnS₄ + ZnS → Cu₂ZnSnS₄ + FeS. It is worth noting that the analyzed sphalerite from the kësterite/ferrokësterite-sphalerite mineral assemblage indicates a deficit in Zn and related metals (Fe, Cu, Mn, Cd, Sn), i.e., a measured average 66.00 wt% vs. The ideal 67.10 wt%, which is likely related to Zn migration from sphalerite to stannite.

Taylor [64] points out that interaction between a complex Sn-Fe-Cu sulfide (e.g., stannite) and an acid solution (O₂-rich) leads to remobilization of Cu, Fe, and Zn with the formation of Fe oxides/hydroxides and Cu minerals in the alteration zone. This process is likely responsible for the presence of finely-intergrown mixtures of emplectite-(kësterite/ferrokësterite)-Fe-oxides/hydroxides, and for the presence of digenite associated with minor covellite.

Kësterite-ferrokësterite and stannite are commonly associated with sphalerite [60]. This mineral assemblage represents a complex system, which apparently formed simultaneously, with no replacement or exsolution textures. The ferrokësterite-kësterite relationships and the chemical character of the Sn-minerals-bornites-phalerite mineral assemblage from the Blidar Contact orebody likely reflect the Zn enrichment/Fe depletion of ferrokësterite to form kësterite, and apparently also Sn migration from ferrokësterite/kësterite to bornite and sphalerite. Simultaneously, Zn migrated from sphalerite to ferrokësterite and contributed to the formation of kësterite, and Cu and Fe migrated from bornite to kësterite, favoring partial replacement of kësterite by bornite and the likely preservation of relict Sn-mineral grains within the newly formed bornite. This interpretation is based on the lack of crystal-structural evidence suggesting that bornite can accommodate concentrations of Sn approaching 10 wt%.

Ferrokësterite, or the so-called zincian-stannite of Springer [49], was considered by this author to be a possible geothermometer if this mineral phase coexists with stannite. According to Shimizu and Shikazono [65], EPMA data on samples that show subsolidus phenomena and a disequilibrium texture are unsuitable for geothermometry use. Co-existing Sn-bearing minerals and sphalerite have been used as a reliable geothermometer based on Fe and Zn partitioning [63,65–67] according to the reaction Cu₂FeSnS₄ (in stannite) + ZnS (in sphalerite) ↔ Cu₂ZnSnS₄ (in stannite) + FeS (in sphalerite), which is valid for all the minerals from the stannite group. For this reaction a K_d partition coefficient is calculated by the formula $K_d = (Fe/Zn)_{stannite}/(Fe/Zn)_{sphalerite}$ [63,66]. The temperature estimation

of the stannite-sphalerite system was experimentally determined and approximated according to the Equations (1) (by Nekrasov et al. [63]) and Equation (2) (by Nakamura and Shima [66]):

$$\log K_d = -1274/T + 1.174 \quad (1)$$

$$\log K_d = -2800/T + 3.5 \quad (2)$$

where T is the temperature in Kelvin.

Osadchiy et al. [68] state that accurate results can be obtained when the data used for the temperature estimation are acquired from mineral grains located at a maximum of 10 μm away from the sphalerite-stannite contact. In contrast, Shimizu and Shikazano [65] claimed that reliable results are obtained by the analyses performed on mineral grains located at least 30 μm away from the stannite-sphalerite contact. Equations (1) and (2) have been used to calculate the temperatures of both the co-existing ferrokösterite and sphalerite and kösterite and sphalerite pairs. No EPMA data is available for the sphalerite associated with stannite. The kösterite, ferrokösterite, and sphalerite EPMA data points considered further for the temperature calculations are located in the vicinity of the kösterite/ferrokösterite-sphalerite contact at a distance ranging between 3–13 μm for kösterite; 6–9 μm for ferrokösterite; and 4–5 μm for sphalerite in the polished section plan. The calculated temperature for the kösterite-sphalerite pair is 503 ± 68 °C according to Equation (1), and 447 ± 17 °C according to Equation (2). The calculated temperature for the co-existing ferrokösterite-sphalerite is 287 ± 25 °C according to Equation (1), and 310 ± 35 °C according to Equation (2).

Partitioning of Zn and Fe between Sn-minerals (stannite and/or ferrokösterite) and sphalerite by several authors yielded comparable results to at least those obtained for the ferrokösterite-sphalerite assemblage from Băița-Bihor: 240–370 °C in the Artana, >340 °C in the Kizhnica, 245–295 °C in the Drazhnje, and 240–390 °C in the Stan Terg ore deposits from the Trepça Pb-Zn mineral belt, Kosovo [69]; 250–350 °C in Japanese skarn and vein deposits [65]; 270–290 °C in the San Rafael lode-type Sn-Cu deposit from Peru [67]; and 300–340 °C in the Otage kaolin-pyrophyllite deposit, Japan [57].

Temperature estimates based on the ferrokösterite-sphalerite pair for the Blidar Contact orebody from Băița-Bihor range from 287 ± 25 °C to 310 ± 35 °C, close to the available data from the literature cited above. Estimated temperatures based on kösterite-sphalerite pair range from 447 ± 17 °C to 503 ± 68 °C, closer to the high temperature estimated for Antoniu North (>400 °C [3]) and Antoniu (~500 °C [37,70]) orebodies.

5.5. Fe-oxides/Hydroxides

The mineral assemblage from the Blidar Contact orebody also contains Fe-oxides/hydroxides. These minerals mainly occur along fissures and mutual grain boundaries between different minerals, e.g., bornite, wittichenite, sphalerite, and galena. They likely formed during the retrograde skarn stage with the release of abundant fluids into the mineralizing system [2]. Iron-oxides/hydroxides are hosted by almost all identified sulfides, with a higher frequency for bornite and wittichenite (Figure 4c). Fe-oxides/hydroxides are also present at sphalerite-bornite contacts (Figures 4f and 5d) and are located along the boundary of bornite grains associated with digenite and minor covellite, and locally, also kösterite-ferrokösterite. In an acid environment, Fe ions released from chalcopyrite may migrate toward the grain border and form a superficial magnetite layer [71], or can be released from the system [72]. Due to iron migration, the remaining bulk particles possess an iron deficit with a composition close to bornite or even covellite [72].

6. Conclusions

Bornite is the main sulfide in the Blidar Contact, Antoniu, and Antoniu North orebodies from the Băița-Bihor skarn deposit. New EPMA data confirm the occurrence of stannite and support the first mention of kösterite and ferrokösterite in the deposit. Bismuth-bearing minerals, i.e., wittichenite, emplectite, joséite-B, and native bismuth are relatively common, especially in the Blidar Contact

orebody. Locally, the Cu-Bi sulfosalts and tellurides are concentrated around native bismuth and occur according to the outward zonality: native bismuth/joséite-B → emplectite → wittichenite. Part of the wittichenite and emplectite formed as a result of the reaction between bornite and native bismuth.

Native gold and electrum were microscopically identified in the Antoniu North ore body in association with hessite and wittichenite hosted by bornite and also in association with chalcopyrite hosted by sphalerite.

The use of ferrokësterite-sphalerite geothermometry constrains the temperature of ore formation in the range of 287 ± 25 °C to 310 ± 35 °C. Application of the kësterite-sphalerite geothermometer yields a somewhat higher temperature (447 ± 17 °C to 503 ± 68 °C).

Supplementary Materials: The following are available online at <http://www.mdpi.com/2075-163X/10/5/436/s1>. Table S1: Analytical conditions for electron probe microanalysis.

Author Contributions: Conceptualization, C.G.T. and M.-P.A.; formal analysis, M.-P.A.; funding acquisition, C.G.T.; investigation, C.G.T. and M.-P.A.; methodology, C.G.T.; resources, C.G.T. and M.-P.A.; supervision, C.G.T.; visualization, M.-P.A.; writing – original draft, M.-P.A.; writing – review & editing, C.G.T. and M.-P.A. All authors have read and agreed to the published version of the manuscript.

Funding: The grants UBB AGC 34718/30.10.2019 and AGC 30104/16.01.2020 (C.G.T.) covered the additional costs of the present work.

Acknowledgments: The present study is the result of a research project conducted by A.M.P. (2017–2018) in the frame of Special scholarships for research, financially supported by the STAR-UBB Institute, Babeş-Bolyai University, Cluj-Napoca. The staff of S.C. Băița S.A. and Vast Resources PLC are highly acknowledged for their support and permission to visit the underground workings in Băița-Bihor. Sándor Mátyási is thanked for his guidance during the field visit. Many thanks to Didier Béziat, GET Laboratory, Toulouse, France and the associated technical staff, Thierry Aigouy (GET, Toulouse), and Philippe de Parseval (UMS 3623 - Centre de MicroCaractérisation Raimond Castaing, Toulouse). Many thanks to Mirela Mircea for the linguistic revision. Extensive review comments by three anonymous reviewers helped improve the clarity of the manuscript.

Conflicts of Interest: The authors declare no conflict of interest.

References

- Berza, T.; Constantinescu, E.; Vlad, Ș.N. Upper Cretaceous magmatic series and associated mineralisation in the Carpathian-Balkan Orogen. *Resour. Geol.* **1998**, *48*, 291–306. [[CrossRef](#)]
- Ciobanu, C.L.; Cook, N.J.; Bogdanov, K.; Kiss, O.; Vuckovic, B. Gold enrichment in deposits of the Banatitic Magmatic and Metallogenic Belt, southeastern Europe. In Proceedings of the Mineral Exploration and Sustainable Development: 7th Biennial SGA Meeting, Athens, Greece, 24–28 August 2003; pp. 1153–1156.
- Cook, N.J.; Ciobanu, C.L.; Danyushevsky, L.V.; Gilbert, S. Minor and trace elements in bornite and associated Cu-(Fe)-sulfides: A LA-ICP-MS study. *Geochim. Cosmochim. Acta* **2011**, *75*, 6473–6496. [[CrossRef](#)]
- Topa, D.; Paar, W.H. Cupromakovickyite, $\text{Cu}_8\text{Pb}_4\text{Ag}_2\text{Bi}_{18}\text{S}_{36}$, a new mineral species of the pavonite homologous series. *Can. Mineral.* **2008**, *46*, 503–514. [[CrossRef](#)]
- Damian, F.; Ciobanu, C.L.; Cook, N.J.; Damian, G. Lead-bismuth sulphotellurides and associated minerals in the Upper Cretaceous Baita Bihor Cu-(Mo) skarn, North Apuseni Mts., Romania. In Proceedings of the Au-Ag-telluride Deposits of the Golden Quadrilateral, Apuseni Mts., Romania. International Field Workshop of IGCP project 486, Alba Iulia, Romania, 31 August–7 September 2004; pp. 221–224.
- Ciobanu, C.L.; Cook, N.J.; Maunders, C.; Benjamin, P.W. Focused Ion Beam and Advanced Electron Microscopy for Minerals: Insights and Outlook from Bismuth Sulphosalts. *Minerals* **2016**, *6*, 112. [[CrossRef](#)]
- Cioflică, G.; Vlad, Ș.; Iosif, V.; Panican, A. Metamorfismul termic și metasomatic al formațiunilor paleozoice din unitatea de Arieșeni de la Băița Bihorului. *Studii și Cercetări de Geologie, Geofizică, Geografie Seria Geologie* **1974**, *19*, 43–68.
- Cioflică, G.; Vlad, Ș.; Volanschi, E.; Stoici, S. Skarnele magneziene cu mineralizațiile asociate de la Băița Bihorului. *Studii și Cercetări de Geologie, Geofizică, Geografie Seria Geologie* **1977**, *22*, 39–57.
- Andrii, M.P.; Tămaș, C.G. Preliminary Mineralogical Data on Bi- and Sn-minerals from Băița Bihor Ore Deposit, North Apuseni Mountains, Romania. In Proceedings of the Sesiunea Științifică Anuală “Ion Popescu Voitești”, Cluj-Napoca, Cluj, Romania, 15 December 2017; pp. 1–8.
- Andrii, M.P.; Tămaș, C.G. Ore mineralogy and geochemistry relationships in Băița Bihor ore deposit, Apuseni Mountains, Romania—Blidar Contact case study. *Romanian J. Mineral Depos.* **2018**, *91*, 49–53.

11. Stoici, S. *Districtul Metalogenetic Băița Bihorului: Cercetări Geologice și Miniere*; Editura Academiei Republicii Socialiste România: Bucharest, Romania, 1983.
12. Udubașa, G. Outstanding mineral occurrences in Romania: What's new? *Acta Mineral. Petrogr.* **2003**, *1*, 106.
13. Papp, G. *History of Minerals, Rocks and Fossil Resins Discovered in the Carpathian Region*; Hungarian Natural History Museum: Budapest, Hungary, 2004.
14. Peters, K.F. *Geologische und Mineralogische Studien aus dem Südöstlichen Ungarn, Insbesondere aus der Umgebung von Rézbánya*; K. K. Hof- und Staastdruckerei: Vienna, Austria, 1861; pp. 385–463.
15. Mumme, W.G.; Žák, L. Padëraite, $\text{Cu}_{5.9}\text{Ag}_{1.3}\text{Pb}_{1.6}\text{Bi}_{11.2}\text{S}_{22}$, a new mineral of the cuprobismutite-hodrushite group. *Neues Jahrb. Mineral. Monatsh.* **1985**, *12*, 557–567.
16. Žák, L.; Fryda, J.; Mumme, W.G.; Paar, W.H. Makovickyite, $\text{Ag}_{1.5}\text{Bi}_{5.5}\text{S}_9$ from Băița Bihorului, Romania. The 4P natural member of the pavonite series. *Neues Jahrb. Mineral. Abh.* **1994**, *168*, 147–169.
17. Ilinca, G.; Makovicky, E.; Topa, D.; Zagler, G. Cuproneite, $\text{Cu}_7\text{Pb}_{27}\text{Bi}_{25}\text{S}_{68}$, a new mineral species from Băița Bihor, Romania. *Can. Mineral.* **2012**, *50*, 353–370. [[CrossRef](#)]
18. Ciobanu, C.L. Grațianite, MnBi_2S_4 , a new mineral from the Băița Bihor skarn, Romania. *Am. Mineral.* **2014**, *99*, 1163–1170. [[CrossRef](#)]
19. Strashimirov, S.; Popov, P. Geology and Metallogeny of the Srednogorie Zone and Panagyurishte Ore Region (Srednogorie Zone, Bulgaria). Guide to excursions A and C. In *ABCD-GEODE Workshop*; Sofia University: Sofia, Bulgaria, 2000.
20. Gallhofer, D.; von Quadt, A.; Peytcheva, I.; Schmid, S.M.; Heinrich, C.A. Tectonic, magmatic, and metallogenic evolution of the Late Cretaceous arc in the Carpathian-Balkan orogen. *Tectonics* **2015**, *34*, 1813–1836. [[CrossRef](#)]
21. Kounov, A.; Schmid, S.M. Fission-track constraints on the thermal and tectonic evolution of the Apuseni Mountains (Romania). *Int. J. Earth Sci.* **2013**, *102*, 207–233. [[CrossRef](#)]
22. Ciobanu, C.L.; Cook, N.J.; Stein, H. Regional setting and geochronology of the Late Cretaceous Banatitic magmatic and metallogenic belt. *Miner. Deposita* **2002**, *37*, 541–567. [[CrossRef](#)]
23. Vlad, Ș.N.; Berza, T. Banatitic magmatic and metallogenic belt: metallogeny of the Romanian Carpathians segment. *Studia UBB Geologia* **2003**, *48*, 113–122. [[CrossRef](#)]
24. Cioflică, G.; Vlad, Ș. The correlation of the Laramian metallogenic events belonging to the Carpatho—Balkan area. *Rev. Roum. Géol. Geoph. Géogr. Géologie* **1973**, *17*, 217–224.
25. Stoici, S. Studiul geologic și petrografic al bazinului superior al Crișului Negru - Băița Bihor cu privire specială asupra mineralizației de bor și a skarnelor magneziene. *Inst. Geol. Geofiz. Stud. Tehn. Econ.* **1974**, *1*, 1–198.
26. Bordea, S.; Dimitrescu, R.; Mantea, G.; Ștefan, A.; Bordea, J.; Bleahu, M.; Costea, C. *Harta Geologică a României, sc. 1:50.000, foaia Biharia*; Institutul de Geologie și Geofizică: Bucharest, Romania, 1988.
27. Bleahu, M. Corelarea depozitelor paleozoice din Munții Apuseni. In Proceedings of the Vth Congress of the Carpathian Balkan Geological Association, Bucharest, Romania, 4–9 September 1961; pp. 75–79.
28. Bordea, S.; Bleahu, M.; Bordea, I. Date noi stratigrafice și structurale asupra Bihorului de vest. Unitatea de Următ și Unitatea de Vetre. *Dări de Seamă ale Ședintelor—Institutul de Geologie și Geofizică* **1975**, *11*, 61–83.
29. Arabu, N. La géologie des environs de Băița (département de Bihor). *C. R. des Séances* **1941**, *25*, 47–94.
30. Seghedi, I. 2. Geological evolution of the Apuseni Mountains with emphasis on the Neogene magmatism—A review. In Proceedings of the Au-Ag-telluride Deposits of the Golden Quadrilateral, Apuseni Mts., Romania, Guidebook of the International Field Work of IGCP Project 486, IAGOD Guidebook Series 12. Alba-Iulia, Romania, 7–31 September 2004; Cook, N.J., Ciobanu, C.L., Eds.; pp. 5–23.
31. Stoicovici, E.; Selegean, I. Considerațiuni la cunoașterea magmatismului banatitic din Munții Bihorului. *Studia Universitatis Babeș-Bolyai, Seria Geologia* **1970**, *15*, 3–15.
32. Cioflică, G.; Vlad, Ș.; Stoici, S. Repartition de la mineralization dans le skarn de Băița Bihorului. *Rev. Roum. Géol. Geoph. Géogr. Géologie* **1971**, *15*, 43–58.
33. Gherasi, N. Microfaciesuri, metamorphism termic și metasomatic în bazinul superior al Crișului Negru. *Dări de Seamă ale Ședintelor—Institutul de Geologie* **1967**, *54*, 22–54.
34. Cioflică, G.; Vlad, Ș. Contribution à la connaissance des types structuraux de pyrometasomatites laramiens de Roumanie. *Revue Roumaine de Géologie, Géophysique, Géographie, s. Géologie* **1973**, *17*, 3–14.
35. Cook, N.J.; Ciobanu, C.L. Cerveleite, Ag_4TeS , from three localities in Romania, substitution of Cu, and the occurrence of the associated phase, $\text{Ag}_2\text{Cu}_2\text{TeS}$. *Neues Jahrb. Mineral. Monatsh.* **2003**, *7*, 321–336. [[CrossRef](#)]
36. Meinert, L. Skarns and Skarn Deposits. *Geosci. Canada* **1992**, *19*, 145–162.

37. George, L.; Cook, N.J.; Ciobanu, C.L. Partitioning of trace elements in co-crystallized sphalerite–galena–chalcopyrite hydrothermal ores. *Ore Geol. Rev.* **2016**, *77*, 97–116. [[CrossRef](#)]
38. George, L.; Cook, N.J.; Ciobanu, C.L.; Benjamin, P.W. Trace and minor elements in galena: A reconnaissance LA-ICP-MS study. *Am. Mineral.* **2015**, *100*, 548–569. [[CrossRef](#)]
39. Marincea, Ș. Fluoborite in magnesian skarns from Baita Bihor (Bihor Massif, Apuseni Mountains, Romania). *Neues Jahrb. Mineral. Monatsh.* **2000**, *8*, 351–371.
40. Marincea, Ș. New data on szaibelyite from the type locality, Băița Bihor, Romania. *Can. Mineral.* **2001**, *39*, 111–127. [[CrossRef](#)]
41. Marincea, Ș. Cristalochimie et propriétés physiques des borates magnésiens des skarns de la province banatitiquie de Roumanie. Sciences de la Terre. Ecole Nationale Supérieure des Mines de Saint-Etienne. Ph.D. Thesis, Grenoble INPG, Grenoble, France, 1998.
42. Marincea, Ș.; Dumitraș, D.-G. Contrasting types of boron-bearing deposits in magnesian skarns from Romania. *Ore Geol. Rev.* **2019**, *112*. [[CrossRef](#)]
43. Criddle, A.J.; Stanley, C.J. *Quantitative Data File for Ore Minerals*, 3th ed.; Criddle, A.J., Stanley, C.J., Eds.; Springer: Dordrecht, The Netherlands, 1993.
44. Sugaki, A.; Hayashi, K.; Kitakaze, A. Hydrothermal synthesis and phase relations of the polymetallic sulphide system. In *Materials Science of the Earth's Interior*; Sunagawa, I., Ed.; Terra Scientific Pub. Co.: Tokyo, Japan, 1984; pp. 545–585.
45. Herzig, P.M. A Mineralogical, Geochemical and Thermal Profile Through the Agrokipia “B” Hydrothermal Sulfide Deposit, Troodos Ophiolite Complex, Cyprus. In *Base Metal Sulfide Deposits in Sedimentary and Volcanic Environments*; Friedrich, G.H., Herzig, P.M., Eds.; Springer: Berlin/Heidelberg, Germany, 1988; pp. 182–215.
46. Cook, N.J.; Ciobanu, C.L.; Pring, A.; Skinner, W.; Shimizu, M.; Danyushevsky, L.; Saini-Eidukat, B.; Melcher, F. Trace and minor elements in sphalerite: A LA-ICPMS study. *Geochim. Cosmochim. Acta* **2009**, *73*, 4761–4791. [[CrossRef](#)]
47. Udubașa, G.; Medesan, A.; Ottemann, J. Über Geochemie und Einfluss von Fe, Mn, Cd und Cu auf die Gitterkonstanten natürlicher Zinkblendes. *Neues Jahrb. Mineral. Abh.* **1974**, *121*, 229–251.
48. Springer, G. Electronprobe analyses of stannite and related tin minerals. *Mineral. Mag. J. Mineral. Soc.* **1968**, *36*, 1045–1051. [[CrossRef](#)]
49. Springer, G. The pseudobinary system $\text{Cu}_2\text{FeSnS}_4$ – $\text{Cu}_2\text{ZnSnS}_4$ and its mineralogical significance. *Can. Mineral.* **1972**, *2*, 535–541.
50. Harris, D.C.; Owens, D.R. A stannite-kesterite exsolution from British Columbia. *Can. Mineral.* **1972**, *11*, 531–534.
51. Hall, S.R.; Szymanski, J.T.; Stewart, J.M. Kesterite, $\text{Cu}_2(\text{Zn,Fe})\text{SnS}_4$, and stannite, $\text{Cu}_2(\text{Fe,Zn})\text{SnS}_4$, structurally similar but distinct minerals. *Can. Mineral.* **1978**, *16*, 131–137.
52. Kissin, S.A. A re-investigation of the stannite ($\text{Cu}_2\text{FeSnS}_4$)-kesterite ($\text{Cu}_2\text{ZnSnS}_4$) pseudobinary system. *Can. Mineral.* **1989**, *27*, 689–697.
53. Kissin, S.A.; Owens, D.A.R. The relatives of stannite in the light of new data. *Can. Mineral.* **1989**, *27*, 673–688.
54. Kissin, S.A.; Owens, D.R. New data on stannite and related tin sulphide minerals. *Can. Mineral.* **1979**, *27*, 686–697.
55. Moore, F.; Howie, R.A. Tin-bearing sulphides from St Michael’s Mount and Cligga Head, Cornwall. *Mineral. Mag.* **1984**, *48*, 389–396. [[CrossRef](#)]
56. Bernardini, G.P.; Bonazzi, P.; Corazza, M.; Corsini, F.; Mazzetti, G.; Poggi, L.; Tanelli, G. New data on the $\text{Cu}_2\text{FeSnS}_4$ – $\text{Cu}_2\text{ZnSnS}_4$ pseudobinary system at 750° and 550 °C. *Eur. J. Mineral.* **1990**, *2*, 219–225. [[CrossRef](#)]
57. Watanabe, M.; Hoshino, K.-I.; Myint, K.K.; Miyazaki, K.; Nishido, H. Stannite from the Otoge kaolin-pyrophyllite deposits, Yamagata Prefecture, NE Japan and its genetical significance. *Resour. Geol.* **1994**, *44*, 439–444.
58. Bonazzi, P.; Bindi, L.; Bernardini, G.P.; Menchetti, S. A model for the mechanism of incorporation of Cu, Fe and Zn in the stannite–kesterite series, $\text{Cu}_2\text{FeSnS}_4$ – $\text{Cu}_2\text{ZnSnS}_4$. *Can. Mineral.* **2003**, *41*, 639–647. [[CrossRef](#)]
59. Corazza, M.; Corsini, F.; Tanelli, G. Stannite group minerals: Investigations on stannite and kesterite. *Rend. Soc. Ital. Mineral. Petrol* **1986**, *41*, 217–222.
60. Petruk, W. Tin sulphides from the deposit of Brunswick Tin Mines Limited. *Can. Mineral.* **1973**, *12*, 46–54.
61. Ivanov, V.V.; Pyatenko, Y.A. On the so-called kesterite (kesterite). *Zap. Vses. Mineral. Obshch.* **1958**, *88*, 165–168.

62. Bogdanov, K.; Tsonev, D.; Popov, K. Mineral assemblages and genesis of the Cu-Au epithermal deposits in the southern part of the Panaguyrishte Ore District, Bulgaria. *Bull. Geol. Soc. Greece* **2004**, *36*, 406–415. [[CrossRef](#)]
63. Nekrasov, I.I.; Sorokin, V.I.; Osadchii, E.G. Fe and Zn partitioning between stannite and sphalerite and its application in geothermometry. *Phys. Chem. Earth* **1979**, *11*, 739–742. [[CrossRef](#)]
64. Taylor, R.G. *Geology of Tin Deposits*; Elsevier Science: Amsterdam, The Netherlands, 1979; Volume 1.
65. Shimizu, M.; Shikazono, N. Iron and zinc partitioning between coexisting stannite and sphalerite: A possible indicator of temperature and sulfur fugacity. *Miner. Deposita* **1985**, *20*, 314–320. [[CrossRef](#)]
66. Nakamura, Y.; Shima, H. Fe and Zn partitioning between sphalerite and stannite (Abstr.). In *Proceedings of Joint Meeting of Society of Mining Geologists of Japan*; The Japanese Association of Mineralogists, Petrologists and Economic Geologists and the Mineralogical Society of Japan: Sendai, Japan, 1982.
67. Wagner, T.; Mlynarczyk, M.S.J.; Williams-Jones, A.E.; Boyce, A.J. Stable isotope constraints on ore formation at the San Rafael tin-copper deposit, Southeast Peru. *Econ. Geol.* **2009**, *104*, 223–248. [[CrossRef](#)]
68. Osadchii, Y.G.; Sorokin, V.I.; Gorbachev, N.S.; Nikulin, V.N. *Physicochemical Conditions of Formation of Sulfide-Oxide Tin Mineralization*; Nauka Press: Moscow, Russia, 1983; pp. 180–194.
69. Kołodziejczyk, J.; Pršek, J.; Voudouris, P.; Melfos, V.; Asllani, B. Sn-bearing minerals and associated sphalerite from lead-zinc deposits, Kosovo: An electron microprobe and LA-ICP-MS study. *Minerals* **2016**, *6*, 42. [[CrossRef](#)]
70. George, L.; Cook, N.J.; Bryony, B.P.C.; Ciobanu, C.L. Trace elements in hydrothermal chalcopyrite. *Mineral. Mag.* **2018**, *82*, 59–88. [[CrossRef](#)]
71. Stefanova, V.; Genevski, K.; Stefanov, B. Mechanism of oxidation of pyrite, chalcopyrite and bornite during flash smelting. *Can. Metall. Q.* **2004**, *43*, 78–88. [[CrossRef](#)]
72. Majuste, D.; Ciminelli, V.S.T.; Osseo-Asare, K.; Dantas, M.S.S.; Magalhães-Paniago, R. Electrochemical dissolution of chalcopyrite: Detection of bornite by synchrotron small angle X-ray diffraction and its correlation with the hindered dissolution process. *Hydrometallurgy* **2012**, *111*, 114–123. [[CrossRef](#)]



© 2020 by the authors. Licensee MDPI, Basel, Switzerland. This article is an open access article distributed under the terms and conditions of the Creative Commons Attribution (CC BY) license (<http://creativecommons.org/licenses/by/4.0/>).